





## Article

# Exploration of Multiple Transfer Phenomena within Viscous Fluid Flows over a Curved Stretching Sheet in the Co-Existence of Gyrotactic Micro-Organisms and Tiny Particles

Pachiyappan Ragupathi <sup>1,†</sup> , N. Ameer Ahammad <sup>2</sup>, Abderrahim Wakif <sup>3</sup> , Nehad Ali Shah <sup>4,†</sup>  and Yongseok Jeon <sup>5,\*</sup> 

<sup>1</sup> Department of Mathematics, Sri Ramakrishna Mission Vidyalaya College of Arts and Science, Coimbatore 641020, India

<sup>2</sup> Department of Mathematics, Faculty of Science, University of Tabuk, P.O. Box 741, Tabuk 71491, Saudi Arabia

<sup>3</sup> Laboratory of Mechanics, Faculty of Sciences Ain Chock, Hassan II University of Casablanca, Casablanca 20000, Morocco

<sup>4</sup> Department of Mechanical Engineering, Sejong University, Seoul 05006, Korea

<sup>5</sup> Interdisciplinary Major of Maritime AI Convergence, Department of Mechanical Engineering, Korea Maritime & Ocean University, Busan 49112, Korea

\* Correspondence: ysjeon@kmou.ac.kr

† These authors contributed equally to this work and are co-first authors.

**Abstract:** In the present study, the magnetohydrodynamics (MHD) bio-convective flow and heat transfer of nanofluid, due to the swimming of the gyrotactic micro-organisms over a curved stretched sheet, is examined. In addition, thermophoresis and Brownian motion behaviors are also investigated by assuming slip conditions at the boundary. A non-linear system of partial differential equations (PDEs) is reduced to a system of ordinary differential equations (ODEs). For convergent solutions, the obtained ODE system is solved by the use of the BVP4C routine integrated MATLAB package. In addition, the impacts of different influential parameters on motile micro-organisms, temperature, velocity, and concentration profiles are deliberated. The velocity field is observed to be reduced when the slip parameter increases. As the main results, it is demonstrated that the distribution of motile microorganisms against the curvature parameter decreases significantly. Similarly, it is found that the nanofluid parameters (i.e., Brownian motion and thermophoresis parameters) and the Peclet number reduce the motile micro-organisms' number. On the other hand, it is evidenced that the motile micro-organisms' distribution can be improved with an increase in bio-convective Schmidt number.

**Keywords:** bio-convection; gyrotactic micro-organisms; curved stretching sheet; slip condition; thermophoresis; Brownian diffusion

**MSC:** 76D05; 82D80



**Citation:** Ragupathi, P.; Ahammad, N.A.; Wakif, A.; Shah, N.A.; Jeon, Y. Exploration of Multiple Transfer Phenomena within Viscous Fluid Flows over a Curved Stretching Sheet in the Co-Existence of Gyrotactic Micro-Organisms and Tiny Particles. *Mathematics* **2022**, *10*, 4133. <https://doi.org/10.3390/math10214133>

Academic Editors: Camelia Petrescu, Valeriu David and Efstratios Tzirtzilakis

Received: 16 September 2022

Accepted: 2 November 2022

Published: 5 November 2022

**Publisher's Note:** MDPI stays neutral with regard to jurisdictional claims in published maps and institutional affiliations.



**Copyright:** © 2022 by the authors. Licensee MDPI, Basel, Switzerland. This article is an open access article distributed under the terms and conditions of the Creative Commons Attribution (CC BY) license (<https://creativecommons.org/licenses/by/4.0/>).

## 1. Introduction

It is well known that magnetohydrodynamics (MHD) is a concept common to both Physics and Mathematics that deals with the study of the interactions of magnetic fields in conducting fluids. The involvement of magnetic fields results in forces that in turn affect the fluid. The structure and intensity of the magnetic fields themselves are therefore possibly altered. The relative performance of the advective movements in the fluid is a key question for a certain conducting fluid experiencing a diffusive impact induced by the resistivity. It also has several application areas such as aerodynamics, life sciences, polymer or fiberglass, cooling systems, exchangers, metallurgy, etc. Hady et al. [1] examined the MHD flow of nanofluid-having gyrotactic micro-organisms with viscous dissipation effects. Pal and Mondal [2] investigated the nanofluid MHD flow with gyrotactic micro-organisms including thermal radiation effects. Yasmin et al. [3] discussed MHD micropolar fluid flows

due to a curved stretching sheet. Nagaraja and Gireesha [4] addressed the MHD flow of Casson fluid. Additionally, the exponential heat generation and chemical reaction effects were also investigated. Few attempts on the topic can be mentioned in the studies [5–8].

Bio-convection results from the upward-swimming of an average number of micro-organisms that are heavier than water. The swimming micro-organisms are collected at the upper water surface. When the collected layer of micro-organisms becomes thicker and thicker, the surface becomes unstable. As a result, a large portion of the gathering falls deeper into the water. This process is repeated by the micro-organisms, and eventually results in bio-convection. Kessler [9] was the person who first noticed and studied the gyrotaxis of microbes. Recently, it has been discovered that several significant phenomena are dependent on the gyrotaxis of microorganisms. These physical phenomena include accumulation at free water surfaces [10], turbulent channel flows in photobioreactors [11], the formation of a thin phytoplankton layer brought on by gyrotactic trapping [12], and microscale patches of motile phytoplankton [13]. Alharbi et al. [14] scrutinized the bio-convection caused by gyrotactic micro-organisms present in the magnetic hybrid nanofluid. This study attempted to support the Targeted Drug Delivery (TDD) system. Modal and Pal [15] inspected the influence of variable viscosity in the bio-convection of micro-organisms present in the nanofluid. Bio-convection in the existence of the Marangoni thermo-solutal effect was considered by Kairi et al. [16]. Khan and Nadeem [17] studied the bio-convection of Maxwell nanofluid. The notion of variability in the thermal conductivity model to analyze the bio-convective Williamson nanofluid was looked over by Abdelmalek et al. [18]. Similarly, numerous investigations on the bio-convection of micro-organisms have been addressed by researchers [19–24].

Due to its various applications in the area of research and production, boundary layer flow over-stretching surfaces is an attractive topic for researchers (Wang [25], Noghrehabadi et al. [26], Rauf et al. [27]). Flows generated by fiber spinning, injection molding, glass molding, spray coating, and pulling of rinsed wires, paper, rubber, glass-fiber, polymer sheet production, etc., are some of the useful applications. As an extension of the stretching surface, the current work is connected with the fluid flow through a curved stretching surface grabbing the attention of numerous researchers. Hayat et al. [28] studied the entropy optimization of CNTs (Carbon Nano Tubes) over a curved stretching sheet. Similarly, Raza et al. [29] examined the entropy optimization of Carreau fluid over a curved stretching sheet. A non-Fourier heat flux model was taken up by Madhukesh et al. [30] to investigate the hybrid nanofluid flow. Darcy-Forchheimer flows of CNTs driven by a curved stretching sheet were considered by Gireesha et al. [31]. Stagnation point flow, involving MHD and Joule heating, was demonstrated by Zhang et al. [32]. The latest developments concerning curved stretching sheets are mentioned in Refs [33–38].

The distribution and swimming properties of gyrotactic microorganisms, in a variety of flows, including horizontal shear flow [11], density stratified flow [39], steady vertical flow [12,40], free surface flow [9], Poiseuille flow [9], as well as the flow past a single vertical circular cylinder [41], have all been the subject of extensive research. The findings demonstrate that gravitational torque and the viscous torque, caused by flow shear in a fluid flowing with non-zero vorticity, have an impact on the swimming of gyrotactic phytoplankton species. Although they are crucial for the prediction of the corresponding concentration distribution, the nanofluid flow behavior relating to the swimming characteristics of gyrotactic microorganisms is currently poorly understood, particularly when Brownian diffusion and thermophoresis are combined.

Ultimately, the goal of this research is to investigate the MHD bio-convective heat transfer caused by gyrotactic micro-organism swimming within the nanofluid past a curved stretched sheet. Using the BVP4c integrated MATLAB package, the solutions to the non-linear system of ODEs are solved. Differences in motile microorganisms, temperature, velocity, and concentration profiles are explained in terms of various influencing parameters, via graphs and tables. The manuscript is prepared in such a way that: Section 2 presents the problem formulation. The numerical scheme's validation is explained in

Section 3. Section 4 contains comments on the collected results, while Section 5 has a list of significant observations.

### 2. Problem Formulation

Consider a two-dimensional MHD nanofluid flow conveying nano-sized particles and gyrotactic micro-organisms across a curved surface of radius  $R$ , as seen in Figure 1. Indeed, the curved sheet is stretched linearly along the  $s$ -direction with a variable velocity  $U_w = as$ , in which a velocity slip condition  $U_{slip}$  is imposed at the fluid-solid interface, where  $a$  is a positive constant. In addition, a uniform magnetic flux density  $B_0$  is applied radially on the developed electrically conducting nanofluid flow.

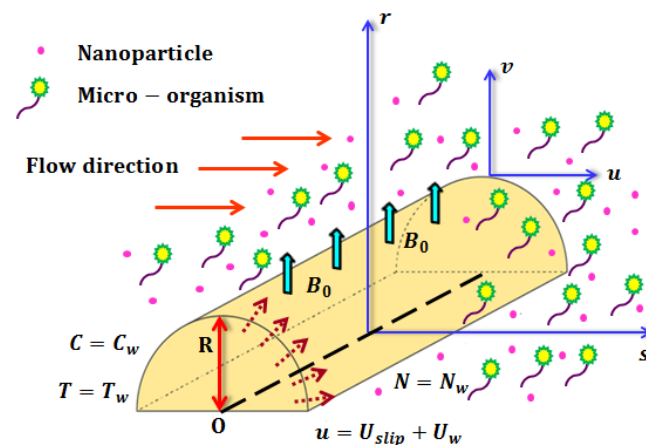


Figure 1. Flow configuration.

The following physical suppositions are adopted:

- The present bio-convective flow is related to a dilute non-homogeneous mixture.
- The studied mixture behaves as an electrically conducting Newtonian media.
- The constituents of the nanofluidic medium are in thermal equilibrium.
- The present MHD non-homogeneous flow is developed in the laminar regime.
- The main governing equations are derived accordingly based on the boundary layer approximations by combining a known non-homogeneous nanofluid model with the conservation equation of gyrotactic micro-organisms.
- As long as the classical formulation of Buongiorno’s approach [42] is adopted as a suitable model to describe the present non-homogeneous nanofluid flow, the thermo-physical expressions of the nanofluid (i.e., density, viscosity, heat capacitance, thermal conductivity, and electrical conductivity) should not be mentioned, because they are included implicitly in the control flow parameters. Therefore, the effects of nanoparticles’ shape and initial volume fraction can be excluded from this investigation.
- In most practical studies, the nanoparticles are prepared in a spherical form.
- Joule heating, Hall current effect, magnetic induction phenomenon, and viscous dissipation are ignored in this investigation as physical constraints.

Based on the aforementioned assumptions, the governing conservation equations are written in the steady state as follows [37]:

$$\frac{\partial v}{\partial r} + \left(\frac{1}{r+R}\right)v + \left(\frac{R}{r+R}\right)\frac{\partial u}{\partial s} = 0, \tag{1}$$

$$\left(\frac{1}{r+R}\right)u^2 = -\frac{1}{\rho}\frac{\partial p}{\partial r}, \tag{2}$$

$$\begin{aligned}
 v \frac{\partial u}{\partial r} + \left(\frac{R}{r+R}\right)u \frac{\partial u}{\partial s} + \left(\frac{1}{r+R}\right)uv &= -\frac{1}{\rho} \left(\frac{R}{r+R}\right) \frac{\partial p}{\partial s} + v \left[ \frac{\partial^2 u}{\partial r^2} + \left(\frac{1}{r+R}\right) \frac{\partial u}{\partial r} - \left(\frac{1}{r+R}\right)^2 u \right] \\
 &\quad - \frac{\sigma}{\rho} B_0^2 u,
 \end{aligned} \tag{3}$$

$$v \frac{\partial T}{\partial r} + \left(\frac{R}{r+R}\right)u \frac{\partial T}{\partial s} = \frac{k}{(\rho C_p)} \left[ \left(\frac{1}{r+R}\right) \frac{\partial T}{\partial r} + \frac{\partial^2 T}{\partial r^2} \right] + \tau \left[ D_B \frac{\partial C}{\partial r} \frac{\partial T}{\partial r} + \frac{D_T}{T_\infty} \left(\frac{\partial T}{\partial r}\right)^2 \right], \tag{4}$$

$$v \frac{\partial C}{\partial r} + \left(\frac{R}{r+R}\right)u \frac{\partial C}{\partial s} = D_B \left[ \left(\frac{1}{r+R}\right) \frac{\partial C}{\partial r} + \frac{\partial^2 C}{\partial r^2} \right] + \frac{D_T}{T_\infty} \left[ \left(\frac{1}{r+R}\right) \frac{\partial T}{\partial r} + \frac{\partial^2 T}{\partial r^2} \right], \tag{5}$$

$$v \frac{\partial N}{\partial r} + \left(\frac{R}{r+R}\right)u \frac{\partial N}{\partial s} = D_m \left[ \left(\frac{1}{r+R}\right) \frac{\partial N}{\partial r} + \frac{\partial^2 N}{\partial r^2} \right] - \frac{bW_c}{C_w - C_\infty} \frac{\partial}{\partial r} \left( N \frac{\partial C}{\partial r} \right), \tag{6}$$

where the symbols  $u$  and  $v$  denote the  $s$ - and  $r$ -velocity components.  $p$  means the pressure,  $\sigma$  is the nanofluid electrical conductivity.  $(\rho C_p)$  reflects the nanofluid heat capacitance.  $D_T$  represents the thermophoresis coefficient.  $T, T_w$  and  $T_\infty$  designate the nanofluid temperature, the wall temperature, and the ambient temperature, respectively.  $D_B$  refers to the coefficient of Brownian diffusion.  $C, C_w$  and  $C_\infty$  indicate the nanofluid concentration (i.e., nanoparticles' volume fraction), the wall concentration, and the ambient concentration, respectively.  $D_m$  signifies the coefficient of motile micro-organisms' diffusion.  $N, N_w$  and  $N_\infty$  stand for the motile micro-organisms' concentration, the motile micro-organisms' concentration at the wall, and the motile micro-organisms' concentration at the ambient region, respectively.  $b$  symbolizes the chemotaxis constant.  $W_c$  marks the maximum cell speed.

For the flow problem the appropriate boundary conditions are:

$$\left\{ \begin{aligned} &u = U_{slip} + U_w, v = 0, T = T_w, C = C_w, N = N_w \text{ at } r = 0, \\ &u \rightarrow 0, \frac{\partial u}{\partial r} \rightarrow 0, T \rightarrow T_\infty, C = C_\infty, N = N_w \text{ as } r \rightarrow \infty \end{aligned} \right\} \tag{7}$$

Here the velocity slip is given by:

$$U_{slip} = \beta \left( \frac{\partial u}{\partial r} - \frac{u}{r+R} \right), \tag{8}$$

where  $\beta$  denotes the slip length.  $\beta = 0$  denotes the no-slip boundary condition. The following new variables are defined to simplify the flow equations:

$$\left\{ \begin{aligned} \eta &= \sqrt{\frac{a}{v}}, F' = \frac{u}{U_w}, F = -\frac{(r+R)}{R\sqrt{av}}v, \theta = \frac{T-T_\infty}{T_w-T_\infty}, \\ \phi &= \frac{C-C_\infty}{C_w-C_\infty}, \chi = \frac{N-N_\infty}{N_w-N_\infty}, P = \frac{p}{\rho U_w^2} \end{aligned} \right\}. \tag{9}$$

Using Equation (9), Equations (1)–(6) takes the following non-dimensional form as follows:

$$P' - \frac{F'^2}{(\eta + A)} = 0, \tag{10}$$

$$F''' + \frac{F''}{(\eta + A)} - \frac{F'}{(\eta + A)^2} + \frac{AFF''}{(\eta + A)} + \frac{AFF'}{(\eta + A)^2} - \frac{AF'^2}{(\eta + A)} - \frac{2AP}{(\eta + A)} - MF' = 0, \tag{11}$$

$$\theta'' + \frac{\theta'}{(\eta + A)} + \frac{PrAF\theta'}{(\eta + A)} + PrNt\theta'^2 + PrNb\theta'\phi' = 0, \tag{12}$$

$$\phi'' + \frac{\phi'}{(\eta + A)} + \frac{ScAF\phi'}{(\eta + A)} + \frac{Nt}{Nb} \left[ \theta'' + \frac{\theta'}{(\eta + A)} \right] = 0, \tag{13}$$

$$\chi'' + \frac{\chi'}{(\eta + A)} + \frac{SbAF\chi'}{(\eta + A)} + Pb[\chi'\phi' + (\tau_0 + \chi)\phi''] = 0 \tag{14}$$

The related boundary conditions in the non-dimensional form are given by:

$$\left\{ \begin{aligned} F = 0, F' = 1 + \beta_1 \left( F'' - \frac{1}{A} F' \right), \theta = \phi = \chi = 1 \text{ at } \eta = 0, \\ F' = F'' = \theta = \phi = \chi = 0 \text{ as } \eta \rightarrow \infty \end{aligned} \right\}. \tag{15}$$

The parameters in non-dimensional forms are represented in Table 1 below:

**Table 1.** Non-dimensional parameters and their related expressions.

Parameters	Expressions	Parameters	Expressions
$M = \frac{\sigma B_0^2}{\rho \alpha}$	Magnetic parameter	$Nb = \frac{\tau_{DB}(C_w - C_\infty)}{v}$	Brownian motion parameter
$A = \sqrt{\frac{a}{v}} R$	Curvature parameter	$Sc = \frac{v}{D_B}$	Schmidt number
$\beta_1 = \beta \sqrt{\frac{a}{v}}$	Slip parameter	$Sb = \frac{v}{D_m}$	Bio-convective Schmidt number
$Pr = \frac{v(\rho C_p)}{k}$	Prandtl Number	$Pb = \frac{bW_c}{D_m}$	Bio-convective Peclet number
$Nt = \frac{\tau_{DT}(T_w - T_\infty)}{vT_\infty}$	Thermophoresis parameter	$\tau_0 = \frac{N_\infty}{N_w - N_\infty}$	Dimensionless bio-convective factor
$Re_s = \frac{U_w s}{v}$	Reynolds number	$\tau = \frac{(\rho C_p)_{np}}{(\rho C_p)}$	Dimensionless thermal factor

The physical quantities of interest are represented as follows:

$$C_f = \frac{\tau_{rs}}{\rho U_w^2}, \text{ where } \tau_w = \mu \left( \frac{\partial u}{\partial r} - \frac{u}{r + R} \right)_{r=0}, \tag{16}$$

$$Nu_s = \frac{sq_w}{k(T_w - T_\infty)}, \text{ where } q_w = -k \left( \frac{\partial T}{\partial r} \right)_{r=0}, \tag{17}$$

$$Sh_s = \frac{sq_j}{D_B(C_w - C_\infty)}, \text{ where } q_j = -D_B \left( \frac{\partial C}{\partial r} \right)_{r=0}, \tag{18}$$

$$Mn_s = \frac{sq_m}{D_m(N_w - N_\infty)}, \text{ where } q_m = -D_m \left( \frac{\partial N}{\partial r} \right)_{r=0}, \tag{19}$$

where  $\tau_w$  represents the surface shear stress.  $q_w$  denotes the wall heat flux.  $q_j$  designates the wall mass flux.  $q_m$  stands for the wall motile micro-organisms' flux. The non-dimensional forms of Equations (16)–(19) are given as:

$$C_f Re_s^{\frac{1}{2}} = F''(0) - \frac{F'(0)}{A}, \tag{20}$$

$$Nu_s Re_s^{-\frac{1}{2}} = -\theta'(0), \tag{21}$$

$$Sh_s Re_s^{-\frac{1}{2}} = -\phi'(0), \tag{22}$$

$$Mn_s Re_s^{-\frac{1}{2}} = -\chi'(0). \tag{23}$$

### 3. Validation

To validate the methodology used in the present study, we compare the obtained results for different values of the slip parameter ( $\beta_1$ ) with those of Wang [24], Noghrehabadi et al. [25], Sahoo and Do [26] and Abbas et al. [37], by assuming that  $M = 0$  and  $A = 1000$ . When the curvature parameter  $A$  tends towards the infinity value, the curved stretching surface is assumed to be a flat stretching surface. Thus, by fixing  $A = 1000$ , the results are found to be in good agreement. The current results are shown in Table 2, which provides

a basis for comparison with Wang [24], Noghrehabadi et al. [25], Sahoo and Do [26], and Abbas et al. [37].

**Table 2.** Comparison of  $C_f Re_s^{\frac{1}{2}}$  for various values of  $\beta_1$ , when  $M = 0$  and  $A = 1000$ .

$\beta_1$	[24]	[25]	[26]	[37]	Present Results
0.0	−1.0	−1.0002	−1.0011	−1.0000	−1.00068
0.1	-	−0.8720	−0.8714	−0.8720	−0.87262
0.2	-	−0.7763	−0.7749	−0.7763	−0.77682
0.3	−0.701	−0.7015	−0.6997	−0.7015	−0.70193
0.5	-	−0.5911	−0.5891	−0.5911	−0.59149
1.0	−0.430	−0.4301	−0.4284	−0.4301	−0.43034
2.0	−0.284	−0.2839	−0.2828	−0.2839	−0.28407
3.0	-	−0.2140	−0.2133	−0.2140	−0.21412
5.0	−0.145	−0.1448	−0.1444	−0.1448	−0.14487
10.0	-	−0.0812	−0.0810	−0.0812	−0.08125
20.0	−0.0438	−0.0437	−0.0437	−0.0437	−0.04379

#### 4. Results and Discussion

The MATLAB software is used herein, through the so-called BVP4C routine, to solve the coupled set of nonlinear ODEs given by Equations (10)–(14) and their accompanying boundary conditions. To achieve mathematical results, we have utilized the following values for various non-dimensional parameters:  $M = 0.5$ ,  $A = 0.5$ ,  $\beta_1 = 1.0$ ,  $Pr = 4.0$ ,  $Nt = 0.2$ ,  $Nb = 0.3$ ,  $Sc = 6.0$ ,  $Sb = 6.0$ ,  $Pb = 0.1$ ,  $\tau_0 = 1$ . With the exception of the modified parameters displayed in the figures, these are maintained as constant. We have discussed the influence of various parameters, such as magnetic parameter ( $M$ ), curvature parameter ( $A$ ), slip parameter ( $\beta_1$ ), thermophoresis parameter ( $Nt$ ), Prandtl number ( $Pr$ ), Brownian motion parameter ( $Nb$ ), bio-convection Schmidt number ( $Sb$ ), Schmidt number ( $Sc$ ), bio-convection Peclet number ( $Pb$ ). Some of these were examined based on the local motile micro-organisms’ number. Table 3 summarizes the values for the physical quantities of interest given in Equations (20)–(23).

**Table 3.** Numerical values of  $C_f Re_s^{\frac{1}{2}}$ ,  $Nu_s Re_s^{-\frac{1}{2}}$ ,  $Sh_s Re_s^{-\frac{1}{2}}$ , and  $Mn_s Re_s^{-\frac{1}{2}}$ .

Parameters	Values	$C_f Re_s^{\frac{1}{2}}$	$Nu_s Re_s^{-\frac{1}{2}}$	$Sh_s Re_s^{-\frac{1}{2}}$	$Mn_s Re_s^{-\frac{1}{2}}$
$M$	0.5	−0.685157	0.341839	1.173836	0.867494
	1.0	−0.737808	0.247285	0.899088	0.583058
	1.5	−0.761642	0.203697	0.790827	0.433161
$A$	1.0	−0.643659	0.312729	1.078490	0.876261
	1.5	−0.612839	0.31028	1.076535	0.903080
	2.0	−0.592397	0.310773	1.081319	0.922313
$\beta_1$	1.0	−0.685157	0.341839	1.173836	0.867494
	1.5	−0.510308	0.284749	0.992354	0.696359
	2.0	−0.406574	0.245495	0.880211	0.574382
$Pr$	3.0	−0.685157	0.353240	1.160884	0.870119
	4.0	−0.685157	0.341839	1.173836	0.867494
	5.0	−0.685157	0.320823	1.192109	0.863649
$Nb$	0.2	−0.685156	0.446899	1.079823	0.888697
	0.3	−0.685157	0.341839	1.173836	0.867494
	0.4	−0.685157	0.258463	1.211724	0.858719
$Nt$	0.2	−0.685157	0.341839	1.173836	0.867494
	0.3	−0.685157	0.299689	1.172226	0.869968
	0.4	−0.685157	0.264082	1.179707	0.870639

Table 3. Cont.

Parameters	Values	$C_f Re_s^{-\frac{1}{2}}$	$Nu_s Re_s^{-\frac{1}{2}}$	$Sh_s Re_s^{-\frac{1}{2}}$	$Mn_s Re_s^{-\frac{1}{2}}$
Sc	5.0	−0.685156	0.360332	1.033888	0.898135
	5.5	−0.685157	0.350414	1.106071	0.882278
	6.0	−0.685157	0.341839	1.173836	0.867494
Sb	5.0	−0.685157	0.341839	1.173836	0.730776
	5.5	−0.685157	0.341839	1.173836	0.801320
	6.0	−0.685157	0.341839	1.173836	0.867494
Pb	0.2	−0.685157	0.341838	1.173835	0.507114
	0.4	−0.685157	0.341838	1.173834	−0.246490
	0.6	−0.685157	0.341838	1.173834	−1.053887

4.1. Curvature Parameter Effects

Figure 2 demonstrates a deteriorating impression of velocity  $F'(\eta)$  when  $A$  becomes larger. Physically, the increasing curvature of the sheet significantly increases the resistance of the flow which slows down the velocity. The same figure shows a similar decreasing pattern for temperature  $\theta(\eta)$ ; as the resistance towards fluid flow is larger for the improving curvature parameter, the concentration of the fluid also improves, which slows the temperature evolution. Figure 3 shows how the nanofluid concentration  $\phi(\eta)$  and the concentration of motile micro-organisms  $\chi(\eta)$  behave as the radius of curvature,  $A$ , increases. As this parameter is increased, the CBL and MMBL are seen to decrease, which is also reflected in the reduction of concentration  $\phi(\eta)$  and concentration of motile micro-organisms  $\chi(\eta)$ .

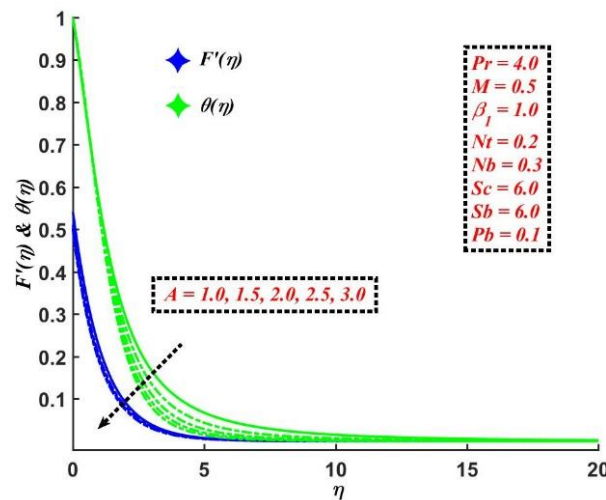


Figure 2. Influence of the curvature parameter on  $F'(\eta)$  and  $\theta(\eta)$ .

4.2. Magnetic Parameter Effects

The effect of the magnetic parameter  $M$  on the dimensionless velocity, temperature, concentration, and concentration of motile micro-organisms' fields are shown in Figures 4 and 5. The magnetic parameter is the proportion of electromagnetic force to inertial force; thus, when  $M$  increases, the velocity field decreases. Due to the presence of a magnetic field, the Lorentz forces are considered to be in hydro-magnetic flow. As  $M$  increases, the strength of the induced magnetic forces increases, with a drop in the velocity field. In addition, the temperature field increases with increasing  $M$  at any point on the BL. This is because when a magnetic field is applied to a flow area, it produces a Lorentz force, which acts as a retarding force, causing the temperature of the fluid inside the BL to rise, as seen in Figure 4. Furthermore, the sheet's surface temperature may be controlled by varying the strength of the applied magnetic field, which also helps in improving the  $\phi(\eta)$  and  $\chi(\eta)$ , as can be seen in Figure 5.



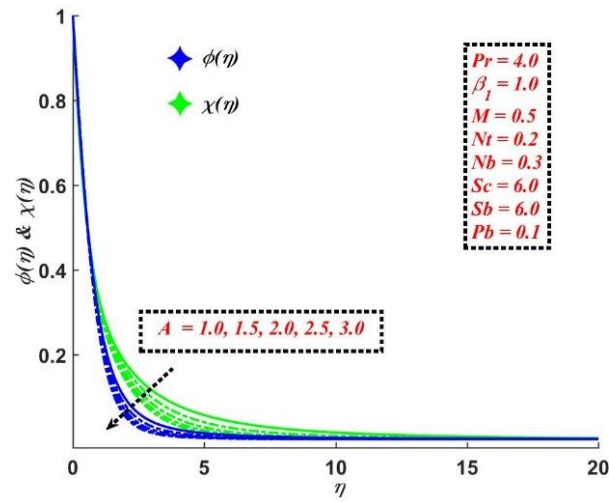


Figure 3. Influence of the curvature parameter on  $\phi(\eta)$  and  $\chi(\eta)$ .

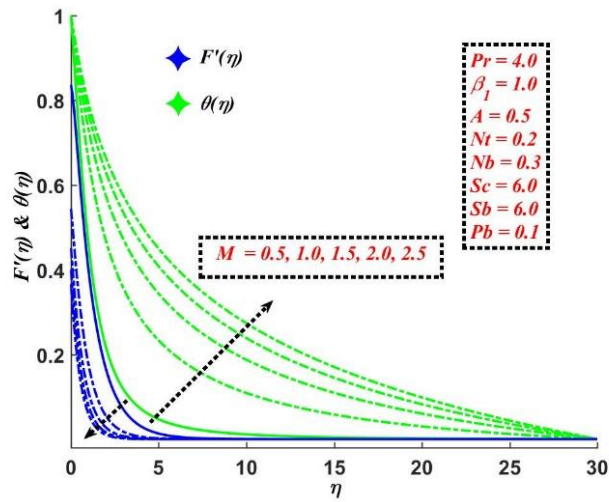


Figure 4. Influence of the magnetic parameter on  $F'(\eta)$  and  $\theta(\eta)$ .

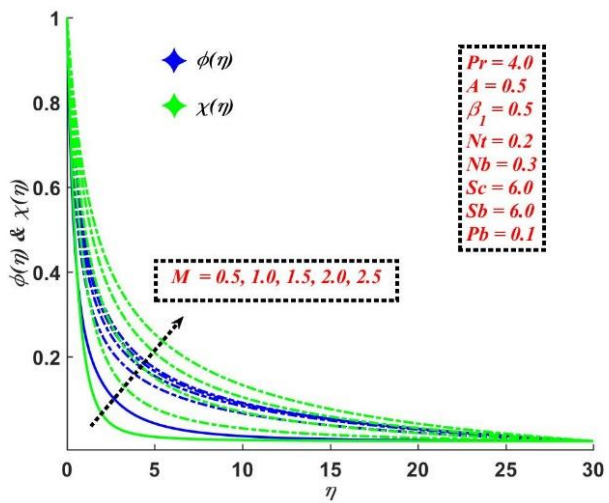


Figure 5. Influence of the magnetic parameter on  $\phi(\eta)$  and  $\chi(\eta)$ .

4.3. Slip Parameter Effects

Figure 6 shows the velocity and temperature fields for varying values of  $\beta_1$ . The velocity decreases as the slip parameter increases, while the temperature increases. This is



because when the slip condition occurs, the stretching sheet’s velocity differs from the flow near the sheet’s velocity. The fluid does not receive a majority of the stretching velocity. As a result, the velocity profile is reduced. In contrast, when  $\beta_1$  is increased, subsequently, the rate of heat transmission from the surface to the ambient fluid is significantly reduced. Thus, the temperature field improves. The same effects are observed for concentration and concentration motile micro-organisms’ profiles in Figure 7. Increases in the slip parameter induce surface friction, which generates a frictional force that causes the particles moving through the fluid to slow down. As a result, the distributions of the nanofluid concentration and the concentration of motile micro-organisms are amplified.

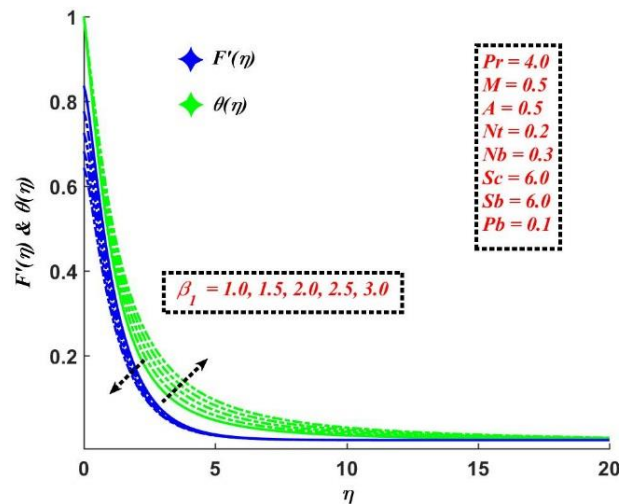


Figure 6. Influence of the slip parameter on  $F'(\eta)$  and  $\theta(\eta)$ .

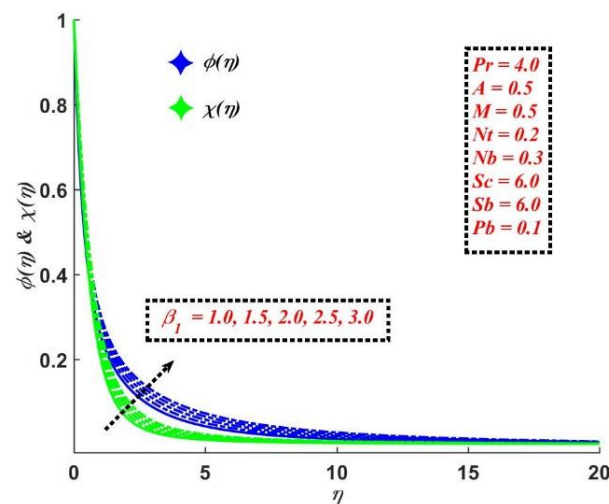


Figure 7. Influence of the slip parameter on  $\phi(\eta)$  and  $\chi(\eta)$ .

#### 4.4. Prandtl Number Effects

Figure 8 shows how different values of the Prandtl number,  $Pr$ , affect the temperature and concentration distribution. As can be seen in Figure 8, increasing the  $Pr$  lowers the temperature and concentration.  $Pr$  is calculated by the amount of momentum to thermal diffusion. As the  $Pr$  rises, thermal and mass diffusion decreases, resulting in a smaller TBL and CBL, as it turned out to reduce  $\theta(\eta)$  and  $\phi(\eta)$ .

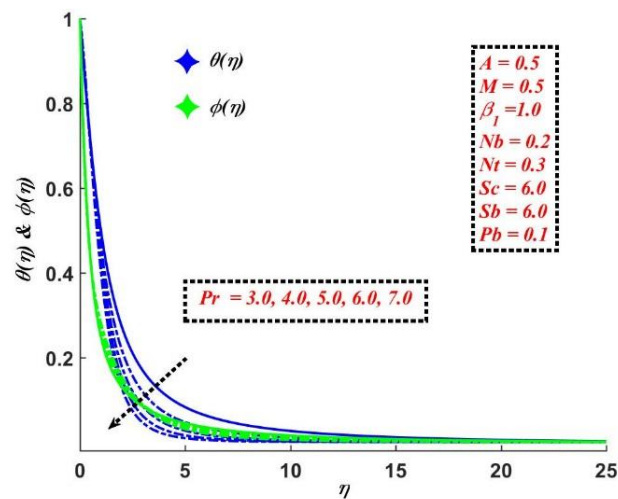


Figure 8. Influence of the Prandtl number on  $\theta(\eta)$  and  $\phi(\eta)$ .

4.5. Thermophoresis and Brownian Motion Parameter Effects

From Figure 9, we can see the behavior of  $Nt$  on  $\theta(\eta)$  and  $\phi(\eta)$ . As is evident in the figure,  $\theta(\eta)$  and  $\phi(\eta)$  are both increased for  $Nt$ . Logically,  $Nt$  determines the intensity of the TBL and CBL. When  $Nt$  rises, the particles begin to move faster, leading to increased kinetic energy within the flow domain; this leads to a rise in  $\theta(\eta)$  and TBL thickness. Similarly, a marginal change in  $Nt$  causes  $\phi(\eta)$  to significantly enhance.

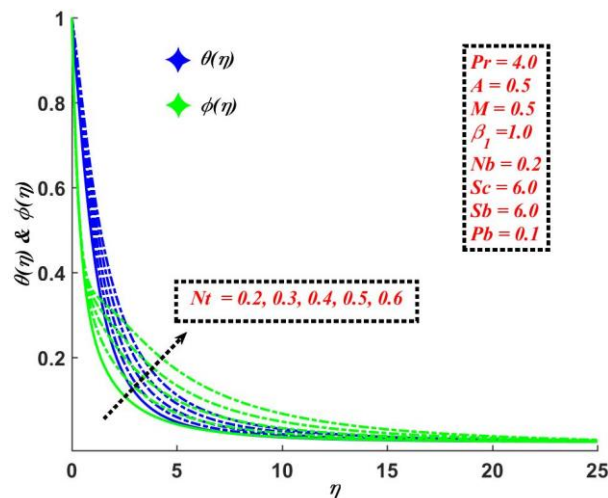


Figure 9. Influence of the thermophoresis parameter on  $\theta(\eta)$  and  $\phi(\eta)$ .

The change in the  $Nt$  causes the fluid particles to move quickly, releasing surplus thermal energy and causing a rise in CBL thickness. As a result,  $\phi(\eta)$ , demonstrated in Figure 10, shows a significant increase. The temperature gradient is significantly affected by the Brownian motion parameter  $Nb$ . When  $Nb$  grows, it produces an increase in  $\theta(\eta)$ , which promotes the TBL thickness. Upgrading  $Nb$  causes faster fluid particle movement, and, as a result, a rise in  $\theta(\eta)$  and TBL thickness is noted, as can be seen in Figure 10. As mentioned earlier, speeding up the particle movement diminishes the concentration gradient; the particles begin to migrate quickly from regions of greater to lower concentration when the mobility of the fluid particles upsurges, with an upsurge in  $Nb$ . Thus, an increase in  $Nb$  causes a drop in  $\phi(\eta)$ , as shown in Figure 10.

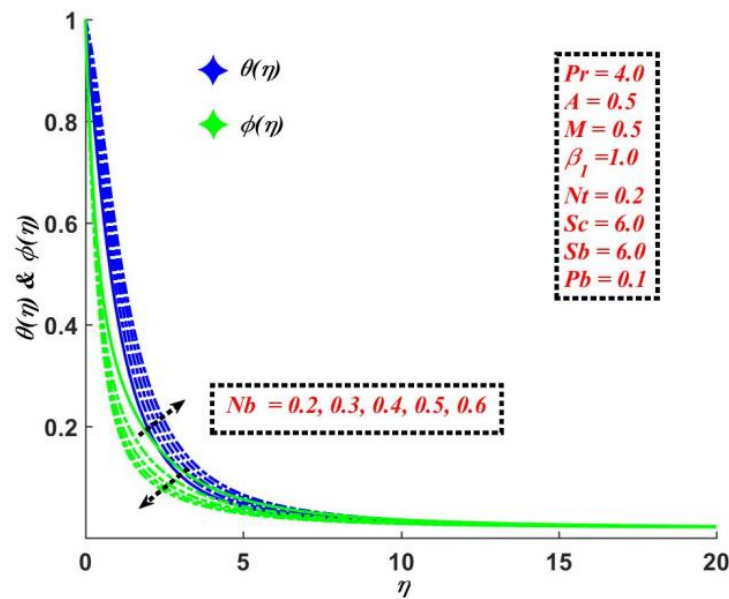


Figure 10. Influence of the Brownian motion parameter on  $\theta(\eta)$  and  $\phi(\eta)$ .

4.6. Schmidt and Peclet Number Effects

The Schmidt number  $Sc$  has a considerable influence on the mass distribution as it increases. Such influence on  $\phi(\eta)$  and  $\chi(\eta)$  is depicted in Figures 11 and 12. The Schmidt number describes the mass momentum transition. It is a physical number that is calculated as the proportion of kinematic viscosity to mass diffusivity in the flow regime, where mass and momentum diffusion circulation mechanisms occur simultaneously. From Figures 11 and 12, it is clear that increasing the Schmidt and bio-convection Schmidt numbers reduces the mass and the micro-organism diffusion and, as a result,  $\phi(\eta)$  and  $\chi(\eta)$  are decreased.

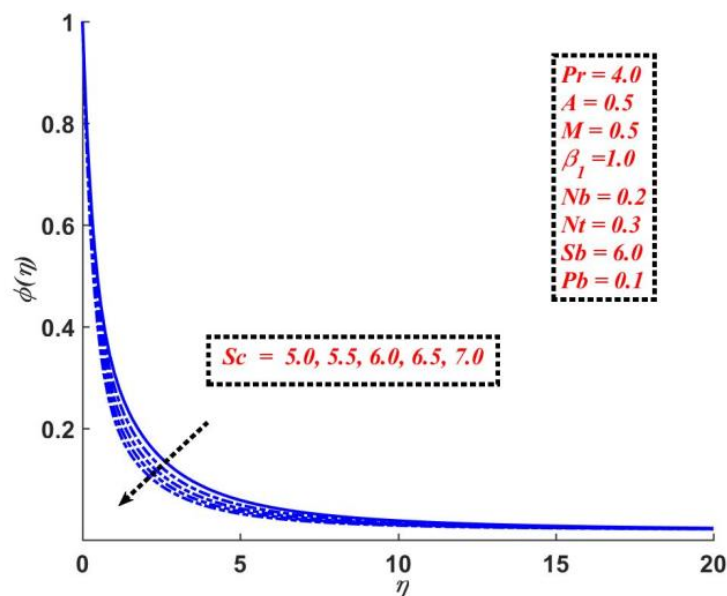


Figure 11. Influence of the Schmidt number on  $\phi(\eta)$ .

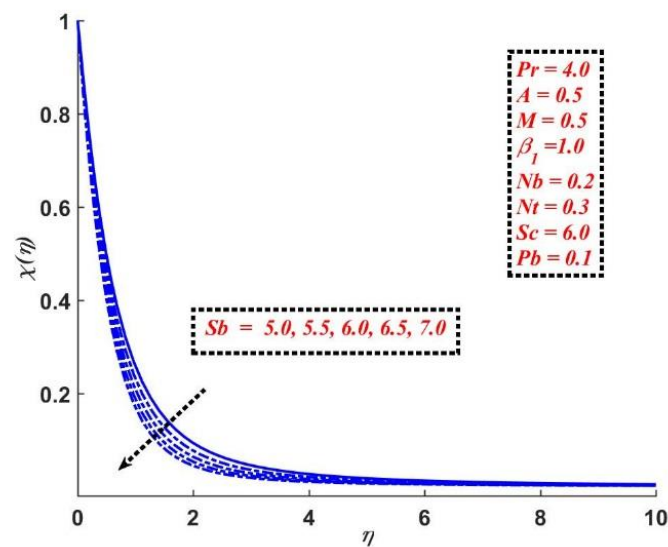


Figure 12. Influence of the bio-convective Schmidt number on  $\chi(\eta)$ .

Figure 13 demonstrates the effect of  $Pb$  on  $\chi(\eta)$ . The increment in  $Pb$  enhances  $\chi(\eta)$ . By using values greater than one and less than one, the estimated Peclet number establishes whether diffusion or convection is the dominant mode of mass movement. Diffusion is a process in which molecules move down a concentration gradient in a net flux. Despite convection being far faster than diffusion, diffusion is the most efficient mode of transport for very small volumes, such as in microfluidic systems. It is noticeable that the diffusion propagation transport is more dominant compared with the advection propagation rate. Hence, by increasing the values of the Peclet number, the motile micro-organisms' profile  $\chi(\eta)$  increases.

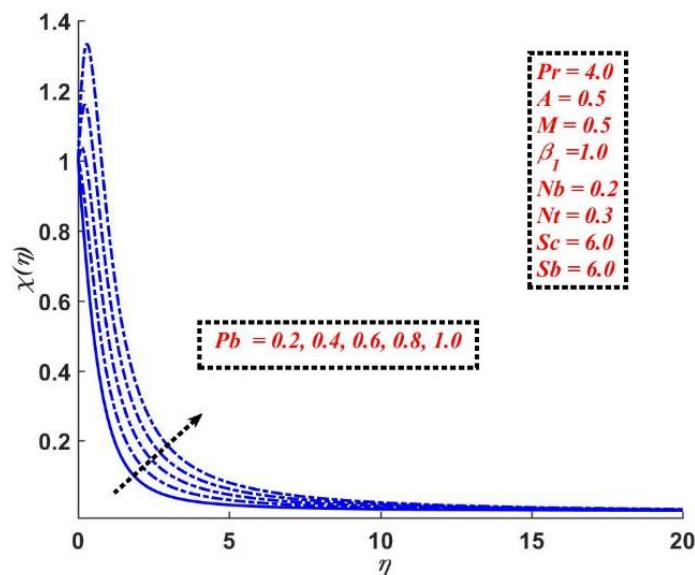


Figure 13. Influence of the bio-convective Peclet number on  $\chi(\eta)$ .

#### 4.7. Effects of Various Parameters on Motile Microorganisms' Number

Figures 14–17 are discussed to show the variations in the micro-organisms' number,  $Mn_s Re_s^{-\frac{1}{2}}$  with  $Nt, Nb, Pb,$  and  $Sb$ . In Figure 14,  $Sb$  is varied between the range  $5 \leq Sb \leq 7$  along the thermophoresis parameter in the range  $0.2 \leq Nt \leq 0.6$ . The variations clearly show that  $Mn_s Re_s^{-\frac{1}{2}}$  decreases for  $Nt$  and increases for  $Sb$ . Similar effects are observed in Figure 15; by fixing the values of  $Sb, Nb$  is changed between  $0.2 \leq Nb \leq 0.6$ . This is because the thermophoretic diffusion and Brownian motion diminish the concentration

of the motile micro-organism gradient of the flowing fluid, as the mobility of the micro-organism increases. The fluctuations in the microorganisms' number with  $Pb$ , along with  $Nt$  and  $Nb$ , are described in Figures 16 and 17. We follow the same range of values for  $Nt$  and  $Nb$ , whereas  $Pb$  is changed between  $0 \leq Pb \leq 1$ . As shown by the fluctuations,  $Mn_s Re_s^{-1/2}$  decreases with  $Nt, Nb$ , and  $Pb$ . For the values  $Pb < 1$  diffusion is more dominant than convection. Hence, we see the micro-organisms' number as a decreasing function.

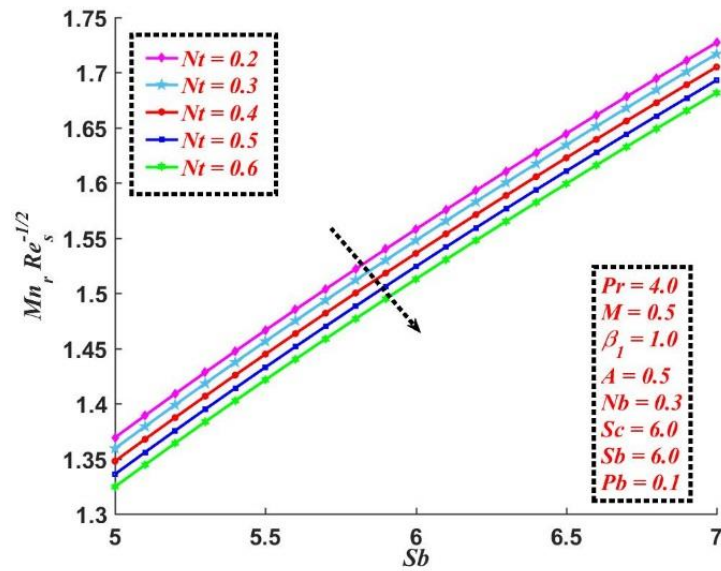


Figure 14. Variation of the motile microorganisms' number with  $Nt$  and  $Sb$ .

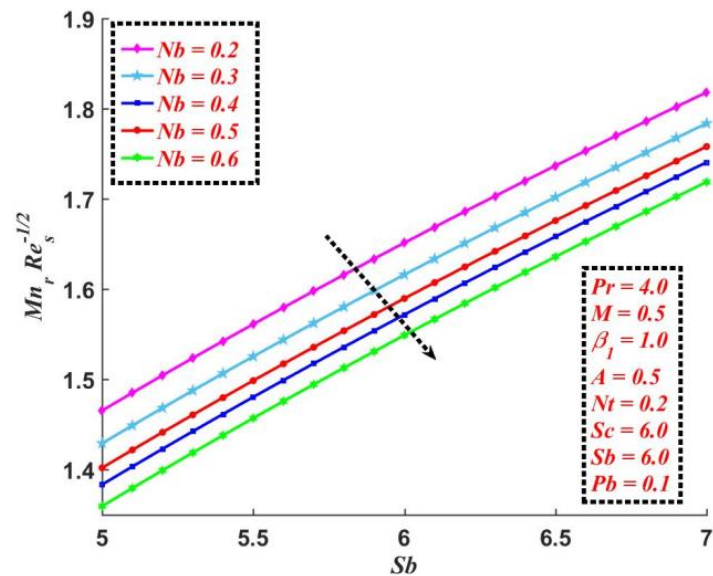


Figure 15. Variation of the motile microorganisms' number with  $Nb$  and  $Sb$ .

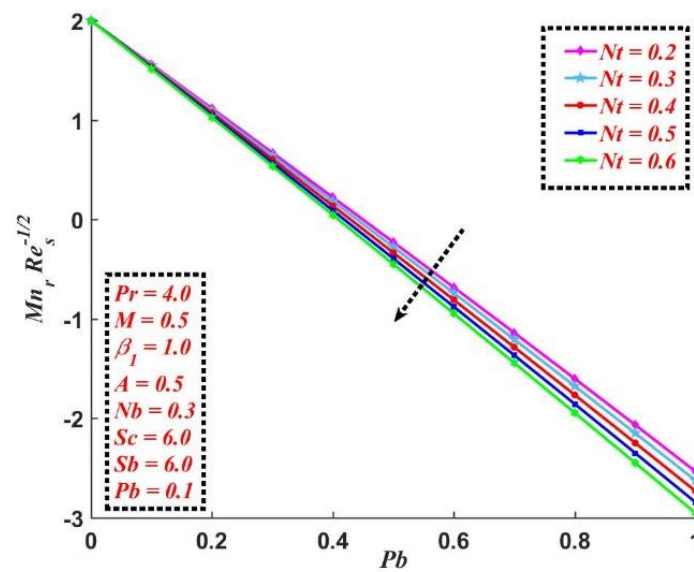


Figure 16. Variation of the motile microorganisms' number with  $Nt$  and  $Pb$ .

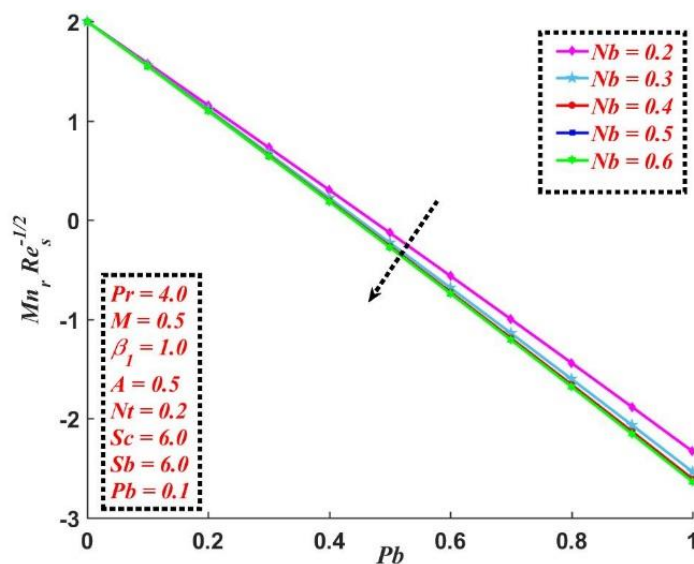


Figure 17. Variation of the motile microorganisms' number with  $Nb$  and  $Pb$ .

### 5. Conclusions

A numerical study is carried out concerning the bio-convection heat transfer of nanofluid flow near a curved stretched sheet containing gyrotactic micro-organisms. This research marks the impact of thermophoresis and Brownian motion in nanofluids that contains both nanoparticles and gyrotactic microorganisms, utilizing the well-known Buongiorno model. Two-dimensional Navier-Stokes, energy, and concentration equations are solved using the BVP4c integrated MATLAB package. The effects of various design parameters on the MHD flow and heat transfer are investigated. The following are the main observations of this study:

- The curvature parameter reduces the profiles of velocity  $F'(\eta)$ , temperature  $\theta(\eta)$ , concentration  $\phi(\eta)$ , and concentration of motile micro-organisms  $\chi(\eta)$ , and their respective boundary layer thicknesses.
- There is a rise in the profiles of temperature  $\theta(\eta)$ , concentration  $\phi(\eta)$ , and concentration of motile micro-organisms  $\chi(\eta)$ , along with a decrement in the velocity profile  $F'(\eta)$  as the magnetic parameter is increased. A similar trend is noticed for the slip parameter.



- The profiles of temperature  $\theta(\eta)$  and concentration  $\phi(\eta)$  tend to diminish due to the impact of the Prandtl number.
- The Brownian motion has opposite effects on the profiles of the temperature  $\theta(\eta)$  (i.e., increasing function) and concentration  $\phi(\eta)$  (i.e., decreasing function). However, the thermophoresis parameter rises the temperature and concentration distributions.
- The increasing values of Schmidt and bio-convection Schmidt numbers decrease the profiles of concentration  $\phi(\eta)$  and concentration of motile micro-organisms  $\chi(\eta)$ .
- The augmenting values of the Peclet number improve significantly the profile of motile micro-organisms' concentration  $\chi(\eta)$ .
- The motile micro-organisms' number is reduced with the increasing values of the Brownian motion parameter, the thermophoresis parameter, and the Peclet number, whereas it enhances with the bio-convection Schmidt number.

Many fields, including pharmacodynamics, drug delivery methods, tumor treatment, hemodynamics, biological polymer synthesis, bacteria-powered micro-mixers, bio-energy systems, pollution dispersion in aquifers, and others [43–47], could benefit from the use of the aforementioned problem. Increasing a nanofluid's stability as a suspension is another justification for including microorganisms in it. The same flagella that propel microorganisms will also cause some mixing at the micro-scale (on a scale that is similar to the size of a nanoparticle and a bacterium), which may prevent nanoparticles from aggregating and agglomerating, and also lead to the macroscopic motion of the host fluid. In this way, the relevance of bioconvection effects in the boundary layer close to the wall has been highlighted by the application of our model to nanofluid heat transfer in the laminar domain.

**Author Contributions:** Conceptualization, P.R., N.A.A., A.W., N.A.S. and Y.J.; methodology, P.R., N.A.A., A.W., N.A.S. and Y.J. software, P.R., N.A.A., A.W., N.A.S. and Y.J.; validation, P.R., N.A.A., A.W., N.A.S. and Y.J.; formal analysis, P.R., N.A.A., A.W., N.A.S. and Y.J.; investigation, P.R., N.A.A., A.W., N.A.S. and Y.J.; resources, P.R., N.A.A., A.W., N.A.S. and Y.J.; writing—original draft preparation, P.R., N.A.A., A.W., N.A.S. and Y.J.; writing—review and editing, P.R., N.A.A., A.W., N.A.S. and Y.J.; visualization, P.R., N.A.A., A.W., N.A.S. and Y.J.; supervision, P.R., N.A.A., A.W., N.A.S. and Y.J.; funding acquisition, Y.J. All authors have read and agreed to the published version of the manuscript.

**Funding:** This study was supported by the National Research Foundation of Korea (NRF) funded by the Korean government (MSIT) [NRF-2021R1I1A3047845, NRF-2022R1A4A3023960] and BK21 Four program through the National Research Foundation of Korea (NRF) funded by the Ministry of Education of Korea (Center for Creative Leaders in Maritime Convergence).

**Data Availability Statement:** Not applicable.

**Conflicts of Interest:** The authors declare no conflict of interest.

## Abbreviations

BL	Boundary Layer
MBL	Momentum Boundary Layer
TBL	Thermal Boundary Layer
CBL	Concentration Boundary Layer
MMBL	Motile Micro-organisms' Boundary Layer



## Nomenclature

### Alphabets

$A$	Curvature parameter
$a$	Stretching rate constant
$b$	Chemotaxis constant
$\{C, C_w, C_\infty\}$	Concentration characteristics
$C_p$	Specific heat capacity
$C_f$	Skin friction coefficient
$D_B$	Brownian diffusion coefficient
$D_T$	Thermophoresis diffusion coefficient
$D_m$	Motile micro-organisms' diffusion coefficient
$\{F, F'\}$	Dimensionless nanofluid velocity components
$k$	Thermal conductivity
$M$	Magnetic parameter
$Mn_s$	Local motile micro-organisms' number
$\{N, N_w, N_\infty\}$	Motile micro-organisms' concentration characteristics
$Nb$	Brownian motion parameter
$Nt$	Thermophoresis parameter
$Nu_s$	Local Nusselt number
$p$	Pressure
$P$	Dimensionless pressure
$Pb$	Bio-convective Peclet number
$Pr$	Prandtl number
$q_w$	Wall heat flux
$q_j$	Wall mass flux
$q_m$	Wall motile micro-organisms flux
$R$	Radius of curvature
$Re$	Reynolds number
$(r, s)$	Curvilinear coordinates
$Sb$	Bio-convective Schmidt number
$Sc$	Schmidt number
$Sh_s$	Local Sherwood number
$\{T, T_w, T_\infty\}$	Temperature characteristics
$U_w$	Stretching sheet velocity
$(u, v)$	$s$ - and $r$ - velocity components
$W_c$	Maximum cell speed

### Greek Letters

$\beta$	Slip length
$\beta_1$	Slip parameter
$\sigma$	Nanofluid's electrical conductivity
$\rho$	Nanofluid's density
$\nu$	Nanofluid's kinematic viscosity
$\mu$	Nanofluid's dynamic viscosity
$\tau_w$	Surface shear stress
$\theta$	Non-dimensional nanofluid temperature
$\phi$	Non-dimensional nanofluid concentration
$\chi$	Non-dimensional motile micro-organisms' concentration
$\eta$	Similarity variable

### Subscripts

$X'$	Ordinary differentiation of $X$ w.r.t $\eta$
------	--

## References

1. Hady, F.M.; Mahdy, A.; Mohamed, R.A.; Zaid, O.A.A. Effects of viscous dissipation on unsteady MHD thermo bioconvection boundary layer flow of a nanofluid containing gyrotactic microorganisms along a stretching sheet. *World J. Mech.* **2016**, *6*, 505–526. [[CrossRef](#)]
2. Pal, D.; Mondal, S.K. MHD nanofluid bioconvection over an exponentially stretching sheet in the presence of gyrotactic microorganisms and thermal radiation. *BioNanoScience* **2018**, *8*, 272–287. [[CrossRef](#)]

3. Yasmin, A.; Ali, K.; Ashraf, M. Study of heat and mass transfer in MHD flow of micropolar fluid over a curved stretching sheet. *Sci. Rep.* **2020**, *10*, 4581. [[CrossRef](#)] [[PubMed](#)]
4. Nagaraja, B.; Gireesha, B.J. Exponential space-dependent heat generation impact on MHD convective flow of Casson fluid over a curved stretching sheet with chemical reaction. *J. Therm. Anal. Calorim.* **2021**, *143*, 4071–4079. [[CrossRef](#)]
5. Haq, F.; Saleem, M.; UR Rahman, M. Investigation of natural bio-convective flow of Cross nanofluid containing gyrotactic microorganisms subject to activation energy and magnetic field. *Phys. Scr.* **2020**, *95*, 105219. [[CrossRef](#)]
6. Koriko, O.K.; Shah, N.A.; Saleem, S.; Chung, J.D.; Omowaye, A.J.; Oreyeni, T. Exploration of bioconvection flow of MHD thixotropic nanofluid past a vertical surface coexisting with both nanoparticles and gyrotactic microorganisms. *Sci. Rep.* **2021**, *11*, 16627. [[CrossRef](#)]
7. Nabwey, H.A.; El-Kabeir, S.M.M.; Rashad, A.M.; Abdou, M.M.M. Effectiveness of Magnetized Flow on Nanofluid Containing Gyrotactic Micro-Organisms over an Inclined Stretching Sheet with Viscous Dissipation and Constant Heat Flux. *Fluids* **2021**, *6*, 253. [[CrossRef](#)]
8. Shah, N.A.; Wakif, A.; El-Zahar, E.R.; Ahmad, S.; Yook, S.-J. Numerical simulation of a thermally enhanced EMHD flow of a heterogeneous micropolar mixture comprising (60%)-ethylene glycol (EG), (40%)-water (W), and copper oxide nanomaterials (CuO). *Case Stud. Therm. Eng.* **2022**, *35*, 102046. [[CrossRef](#)]
9. Kessler, J.O. Hydrodynamic focusing of motile algal cells. *Nature* **1985**, *313*, 218–220. [[CrossRef](#)]
10. Lovecchio, S.; Zonta, F.; Marchioli, C.; Soldati, A. Thermal stratification hinders gyrotactic micro-organism rising in free-surface turbulence. *Phys. Fluids* **2017**, *29*, 053302. [[CrossRef](#)]
11. Croze, O.A.; Sardina, G.; Ahmed, M.; Bees, M.A.; Brandt, L. Dispersion of swimming algae in laminar and turbulent channel flows: Consequences for photobioreactors. *J. R. Soc. Interface* **2013**, *10*, 20121041. [[CrossRef](#)] [[PubMed](#)]
12. Durham, W.M.; Kessler, J.O.; Stocker, R. Disruption of vertical motility by shear triggers formation of thin phytoplankton layers. *Science* **2009**, *323*, 1067–1070. [[CrossRef](#)] [[PubMed](#)]
13. Durham, W.M.; Climent, E.; Barry, M.; Lillo, F.D.; Boffetta, G.; Cencini, M.; Stocker, R. Turbulence drives microscale patches of motile phytoplankton. *Nat. Commun.* **2013**, *4*, 2148. [[CrossRef](#)] [[PubMed](#)]
14. Alharbi, F.M.; Naeem, M.; Zubair, M.; Jawad, M.; Jan, W.U.; Jan, R. Bioconvection Due to Gyrotactic Microorganisms in Couple Stress Hybrid Nanofluid Laminar Mixed Convection Incompressible Flow with Magnetic Nanoparticles and Chemical Reaction as Carrier for Targeted Drug Delivery through Porous Stretching Sheet. *Molecules* **2021**, *26*, 3954. [[CrossRef](#)]
15. Mondal, S.K.; Pal, D. Computational analysis of bioconvective flow of nanofluid containing gyrotactic microorganisms over a nonlinear stretching sheet with variable viscosity using HAM. *J. Comput. Des. Eng.* **2020**, *7*, 251–267. [[CrossRef](#)]
16. Kairi, R.R.; Shaw, S.; Roy, S.; Raut, S. Thermosolutal marangoni impact on bioconvection in suspension of gyrotactic microorganisms over an inclined stretching sheet. *J. Heat Transf.* **2021**, *143*, 031201. [[CrossRef](#)]
17. Khan, M.N.; Nadeem, S. Theoretical treatment of bio-convective Maxwell nanofluid over an exponentially stretching sheet. *Can. J. Phys.* **2020**, *98*, 732–741. [[CrossRef](#)]
18. Abdelmalek, Z.; Khan, S.U.; Waqas, H.; Riaz, A.; Khan, I.A.; Tlili, I. A mathematical model for bioconvection flow of Williamson nanofluid over a stretching cylinder featuring variable thermal conductivity, activation energy and second-order slip. *J. Therm. Anal. Calorim.* **2021**, *144*, 205–217. [[CrossRef](#)]
19. Shafiq, A.; Lone, S.A.; Sindhu, T.N.; Al-Mdallal, Q.M.; Rasool, G. Statistical modeling for bioconvective tangent hyperbolic nanofluid towards stretching surface with zero mass flux condition. *Sci. Rep.* **2021**, *11*, 13869. [[CrossRef](#)]
20. Chu, Y.-M.; ur Rahman, M.; Khan, M.I.; Kadry, S.; Rehman, W.U.; Abdelmalek, Z. Heat transport and bio-convective nanomaterial flow of Walter 's-B fluid containing gyrotactic microorganisms. *Ain Shams Eng. J.* **2021**, *12*, 3071–3079. [[CrossRef](#)]
21. Xia, W.-F.; Haq, F.; Saleem, M.; Khan, M.I.; Khan, S.U.; Chu, Y.-M. Irreversibility analysis in natural bio-convective flow of Eyring-Powell nanofluid subject to activation energy and gyrotactic microorganisms. *Ain Shams Eng. J.* **2021**, *12*, 4063–4074. [[CrossRef](#)]
22. Aneja, M.; Sharma, S.; Kuharat, S.; Beg, O.A. Computation of electroconductive gyrotactic bioconvection from a nonlinear inclined stretching sheet under nonuniform magnetic field: Simulation of smart bio-nanopolymer coatings for solar energy. *Int. J. Mod. Phys. B* **2020**, *34*, 2050028. [[CrossRef](#)]
23. Magagula, V.M.; Shaw, S.; Kairi, R.R. Double dispersed bioconvective Casson nanofluid fluid flow over a nonlinear convective stretching sheet in suspension of gyrotactic microorganism. *Heat Transf.* **2020**, *49*, 2449–2471. [[CrossRef](#)]
24. Manan, A.; Rehman, S.U.; Fatima, N.; Imran, M.; Ali, B.; Shah, N.A.; Chung, J.D. Dynamics of Eyring–Powell Nanofluids When Bioconvection and Lorentz Forces Are Significant: The Case of a Slender Elastic Sheet of Variable Thickness with Porous Medium. *Mathematics* **2022**, *10*, 3039. [[CrossRef](#)]
25. Wang, C.Y. Flow due to a stretching boundary with partial slip—an exact solution of the Navier-Stokes equations. *Chem. Eng. Sci.* **2002**, *57*, 3745–3747. [[CrossRef](#)]
26. Noghrehabadi, A.; Pourrajab, R.; Ghalambaz, M. Effect of partial slip boundary condition on the flow and heat transfer of nanofluids past stretching sheet prescribed constant wall temperature. *Int. J. Therm. Sci.* **2012**, *54*, 253–261. [[CrossRef](#)]
27. Rauf, A.; Mushtaq, A.; Shah, N.A.; Botmart, T. Heat transfer and hybrid ferrofluid flow over a nonlinearly stretchable rotating disk under the influence of an alternating magnetic field. *Sci Rep.* **2022**, *12*, 17548. [[CrossRef](#)]
28. Hayat, T.; Khan, S.A.; Alsaedi, A.; Zai, Q.Z. Computational analysis of heat transfer in mixed convective flow of CNTs with entropy optimization by a curved stretching sheet. *Int. Commun. Heat Mass Transf.* **2020**, *118*, 104881. [[CrossRef](#)]

29. Raza, R.; Mabood, F.; Naz, R. Entropy analysis of non-linear radiative flow of Carreau liquid over curved stretching sheet. *Int. Commun. Heat Mass Transf.* **2020**, *119*, 104975. [[CrossRef](#)]
30. Madhukesh, J.K.; Kumar, R.N.; Gowda, R.J.P.; Prasannakumara, B.C.; Ramesh, G.K.; Khan, M.I.; Khan, S.U.; Chu, Y.-M. Numerical simulation of AA7072-AA7075/water-based hybrid nanofluid flow over a curved stretching sheet with Newtonian heating: A non-Fourier heat flux model approach. *J. Mol. Liq.* **2021**, *335*, 116103. [[CrossRef](#)]
31. Gireesha, B.J.; Nagaraja, B.; Sindhu, S.; Sowmya, G. Consequence of exponential heat generation on non-Darcy-Forchheimer flow of water based carbon nanotubes driven by a curved stretching sheet. *Appl. Math. Mech.* **2020**, *41*, 1723–1734. [[CrossRef](#)]
32. Zhang, X.-H.; Abidi, A.; Ahmed, A.E.-S.; Khan, M.R.; El-Shorbagy, M.A.; Shutaywi, M.; Issakhov, A.; Galal, A.M. MHD stagnation point flow of nanofluid over curved stretching/shrinking surface subject to the influence of Joule heating and convective condition. *Case Stud. Therm. Eng.* **2021**, *26*, 101184. [[CrossRef](#)]
33. Qian, W.-M.; Khan, M.I.; Shah, F.; Khan, M.; Chu, Y.-M.; Khan, W.A.; Nazeer, M. Mathematical Modeling and MHD Flow of Micropolar Fluid Toward an Exponential Curved Surface: Heat Analysis via Ohmic Heating and Heat Source/Sink. *Arab. J. Sci. Eng.* **2021**, *47*, 867–878. [[CrossRef](#)]
34. Afsar Khan, A.; Batool, R.; Kousar, N. Examining the behavior of MHD micropolar fluid over curved stretching surface based on the modified Fourier law. *Sci. Iran.* **2021**, *28*, 223–230. [[CrossRef](#)]
35. Rehman, S.U.; Fatima, N.; Ali, B.; Imran, M.; Ali, L.; Shah, N.A.; Chung, J.D. The Casson Dusty Nanofluid: Significance of Darcy–Forchheimer Law, Magnetic Field, and Non-Fourier Heat Flux Model Subject to Stretch Surface. *Mathematics* **2022**, *10*, 2877. [[CrossRef](#)]
36. Kempnagari, A.K.; Buruju, R.R.; Naramgari, S.; Vangala, S. Effect of Joule heating on MHD non-Newtonian fluid flow past an exponentially stretching curved surface. *Heat Transf.* **2020**, *49*, 3575–3592. [[CrossRef](#)]
37. Asogwa, K.K.; Goud, B.S.; Shah, N.A.; Yook, S.-J. Rheology of electromagnetohydrodynamic tangent hyperbolic nanofluid over a stretching riga surface featuring dufour effect and activation energy. *Sci. Rep.* **2022**, 14602. [[CrossRef](#)]
38. Rasool, G.; Shah, N.A.; El-Zahar, E.R.; Wakif, A. Numerical investigation of EMHD nanofluid flows over a convectively heated riga pattern positioned horizontally in a Darcy-Forchheimer porous medium: Application of passive control strategy and generalized transfer laws. *Waves Random Complex Media* **2022**, 1–20. [[CrossRef](#)]
39. Ardekani, A.M.; Doostmohammadi, A.; Desai, N. Transport of particles, drops, and small organisms in density stratified fluids. *Phys. Rev. Fluids* **2017**, *2*, 100503. [[CrossRef](#)]
40. Lillo, D.F.; Cencini, M.; Durham, W.M.; Barry, M.; Stocker, R.; Climent, E.; Boffetta, G. Turbulent fluid acceleration generates clusters of gyrotactic microorganisms. *Phys. Rev. Lett.* **2014**, *112*, 044502. [[CrossRef](#)]
41. Zeng, L.; Pedley, T.J. Distribution of gyrotactic micro-organisms in complex three-dimensional flows. Part 1. Horizontal shear flow past a vertical circular cylinder. *J. Fluid Mech.* **2018**, *852*, 358–397. [[CrossRef](#)]
42. Buongiorno, J. Convective Transport in Nanofluids. *J. Heat Transf.* **2006**, *128*, 240–250. [[CrossRef](#)]
43. Sokolov, A.; Goldstein, R.E.; Feldchtein, F.I.; Aranson, I.S. Enhanced mixing and spatial instability in concentrated bacterial suspensions. *Phys. Rev. E* **2009**, *80*, 031903. [[CrossRef](#)] [[PubMed](#)]
44. Tsai, T.-H.; Liou, D.-S.; Kuo, L.-S.; Chen, P.-H. Rapid mixing between ferro-nanofluid and water in a semi-active Y-type micromixer. *Sens. Actuators A Phys.* **2009**, *153*, 267–273. [[CrossRef](#)]
45. Uddin, M.J.; Khan, W.A.; Qureshi, S.R.; Beg, O.A. Bioconvection nanofluid slip flow past a wavy surface with applications in nano-biofuel cells. *Chin. J. Phys.* **2017**, *55*, 2048–2063. [[CrossRef](#)]
46. Shaijumon, M.M.; Ramaprabhu, S.; Rajalakshmi, N. Platinum/multiwalled carbon nanotubes–platinum/carbon composites as electrocatalysts for oxygen reduction reaction in proton exchange membrane fuel cell. *Appl. Phys. Lett.* **2006**, *88*, 253105. [[CrossRef](#)]
47. Naskar, S.; Sharma, S.; Kuotsu, K. Chitosan-based nanoparticles: An overview of biomedical applications and its preparation. *J. Drug Deliv. Sci. Technol.* **2019**, *49*, 66–81. [[CrossRef](#)]